

# SIZE BASED NANOPARTICLE SEPARATION USING DIELECTROPHORETIC FOCUSING FOR FEMTOSECOND NANOCRYSTALLOGRAPHY OF MEMBRANE PROTEINS

Bahige Abdallah, Tzu-Chiao Chao, Petra Fromme, Alexandra Ros

*Department of Chemistry and Biochemistry, Arizona State University, Tempe, AZ, USA*

## ABSTRACT

We propose a method to separate photosystem I crystals based on size using a combination of dielectrophoresis (DEP) and electrokinesis (EK) within a microfluidic device. In this work, a model system utilizing polystyrene beads of two sizes is employed to observe the effects of DEP and EK on particles as they pass through a microsorter via electroosmosis. Particle counting and fluorescence intensity measurements are used for quantitative analysis of experimental data. For comparison, numerical simulations were performed for further confirmation that the proposed device is capable of sorting particles based on their size. Our experimental and theoretical results are in agreement and show a high degree of sorting efficiency between both particle types making this a promising solution for protein crystal sorting.

## KEYWORDS

Dielectrophoresis, Microfluidics, Separation, Nanoparticle, Crystallography

## INTRODUCTION

Our work improves upon existing sorting devices for beads [1] by tuning dielectrophoretic focusing versus electrokinetic forces. Thereby we improve this methodology to sort membrane protein crystals on the order of 100 nm in diameter. Femtosecond nanocrystallography is an emerging technique with the potential to obtain structural information for membrane proteins without the need of growing large crystals [2]. The latter represents the major challenge in membrane protein structure elucidation as membrane proteins are difficult to grow in large sizes suitable for conventional X-ray structure determination. However, due to the heterogeneity inherent to current crystallization techniques for membrane proteins, nanocrystallography experiments are hampered by broad size distributions obtained among smaller crystals. Further downstream processing to isolate a desired crystal size and improve monodispersity is necessary and addressed in the presented work.

## THEORY

To drive size based separation, the size dependency of DEP is exploited. It is first important to consider the DEP velocity ( $\vec{u}_{DEP}$ ) experienced by a spherical particle, which is directly related to the electric field gradient ( $\nabla E^2$ ) and DEP mobility ( $\mu_{DEP}$ ):

$$\vec{u}_{DEP} = -\mu_{DEP} \nabla E^2 \quad (1)$$

Furthermore, the DEP mobility exhibited by a spherical particle is directly related to its diameter,  $d_p$  [3]:

$$\mu_{DEP} = \frac{\pi d_p^2 f_{cm} \epsilon_m}{12\eta} \quad (2)$$

where  $f_{cm}$  is the Clausius-Mossotti factor,  $\epsilon_m$  is the medium permittivity, and  $\eta$  is the medium viscosity. A system can either exhibit negative or positive DEP based on the sign of the Clausius-Mossotti factor which under DC conditions is determined by medium ( $\sigma_m$ ) and particle ( $\sigma_p$ ) conductivities [4]:

$$f_{cm} = \frac{\sigma_p - \sigma_m}{\sigma_p + 2\sigma_m} \quad (3)$$

Particles with conductivities smaller than their respective media experience negative DEP. In the case of this experiment, negative DEP prevails at a  $\sigma_m$  of  $\sim 10^{-3}$  S/m thus particles of increasing size are deflected more strongly from regions of high electric field gradients. We study the DEP sorting in a device (Figure 1) consisting of an inlet channel in which a bulk crystal solution can be injected. An insulator constriction is positioned between the inlet and outlet channels to create a heterogeneous electric field in the longitudinal direction evoking DEP as particles migrate through the microchannel. Upon entering the restriction region, larger particles are repelled from the channel walls due to negative DEP and focus in the center of the microdevice. Conversely, smaller particles experiencing weaker repulsion are prone to deflection into a series of outlet channels for effective sorting. Figure 2 illustrates the variable electric field gradients throughout the microchannel facilitating particle DEP behavior patterns for sorting into collection channels.

## EXPERIMENTAL

The microstructure design was developed using CAD software from which a Cr mask was created. Photolithography was employed to transfer structures to a silicon master wafer with negative photoresist and a mold fabricated using poly(dimethylsiloxane) (PDMS). Reservoirs were punched into channel ends and the PDMS mold was sealed to a glass slide via oxygen plasma treatment. HEPES buffer ( $1.5 \times 10^{-3}$  S/m, pH 5) with F108 blocking agent is flushed through the channels to dynamically coat channel walls and reduce adsorption. Polystyrene beads ( $1 \mu\text{m}$  and  $0.1 \mu\text{m}$ , Spherotech) suspended in the same buffer are added to the inlet reservoir and DC potentials are applied to the microdevice reservoirs to induce electroosmotic flow (EOF) as well as electric field gradients at the constriction region for dielectrophoretic focusing. Fluorescence microscopy imaging was performed using a CCD camera coupled to a beamsplitter to segregate the fluorescence response of each bead type. Fluorescence intensity was measured using ImageJ software to quantify the relative concentration of the  $0.1 \mu\text{m}$  beads in each outlet.  $1 \mu\text{m}$  bead data was analyzed by particle tracing using an ImageJ plugin. Particles were counted as they passed through the center (C), the mid-outer (MO), and outer (O) outlets separately using a detection window with an area of  $\sim 100 \mu\text{m}^2$ . Numerical simulations were performed using *Comsol Multiphysics 4.3*.

## RESULTS AND DISCUSSION

We demonstrate that the potential in the outlet reservoirs is a major driving force for sorting and dielectrophoretic focusing. Experimentally, the optimal potential scheme is 10V inlet,  $-55 \pm 5\text{V}$  center outlet, and  $-20\text{V}$  to the remaining outlets. We follow the bead migration by using beads with two distinct fluorescence characteristics simultaneously and monitor their migration. Figure 3 shows the experimentally observed fractionation of nano- and microbeads with excellent selectivity for  $0.1 \mu\text{m}$  beads. At  $-55 \pm 5\text{V}$  applied to the center outlet, the  $0.1 \mu\text{m}$  beads disperse into all outlets (Figure 3b) whereas at higher potentials they focus on the center outlet (Figure 3a). In comparison to the  $1 \mu\text{m}$  beads at the same applied potentials, we see focusing on the center channel exclusively (Figure 3c). This leads to the separation of  $0.1 \mu\text{m}$  beads into the offset outlets away from the larger beads present in solution.

To quantify experimental data, fluorescence intensity was measured in the center (C), the mid-outer (MO), and outer (O) outlets separately. The data for the  $0.1 \mu\text{m}$  beads was normalized with the highest fluorescence intensity given by the center outlet. As shown in Figure 4, the  $0.1 \mu\text{m}$  beads have a nearly equal distribution into all outlet channels with normalized intensities  $> 0.9$ . Particle counts for the  $1 \mu\text{m}$  beads were normalized by setting the total number of particles to 1 and calculating the relative fraction of particles counted in each of the outlets separately (Figure 4). Our data shows that the  $1 \mu\text{m}$  beads favored the center outlet 82% of the time whereas deflection into the MO and O outlets occurred 15% and 3% of the time, respectively. These quantification results further confirm that  $1 \mu\text{m}$  beads selectively focus into the center outlet whereas  $0.1 \mu\text{m}$  beads distribute into all outlets leading to effective sorting of the differentially sized particles.

Numerical simulations were performed with *Comsol* in order to analyze experimental results within the given device geometry using the Transport of Diluted Species module. We adapt diffusion, EOF, and the dielectrophoretic mobility to the size of the employed particle. These simulations demonstrate specific size selection with  $-50\text{V}$  applied to the center outlet ( $-20\text{V}$  to MO and O outlets) as demonstrated in Figure 5 which is in agreement with experimental results. We furthermore demonstrate that the DEP effect is insignificant for the  $0.1 \mu\text{m}$  beads as the concentration profile considering DEP shown in Figure 5a is identical to that without DEP (not shown). In both cases, the concentration profile is relatively constant for all outlets as expected.

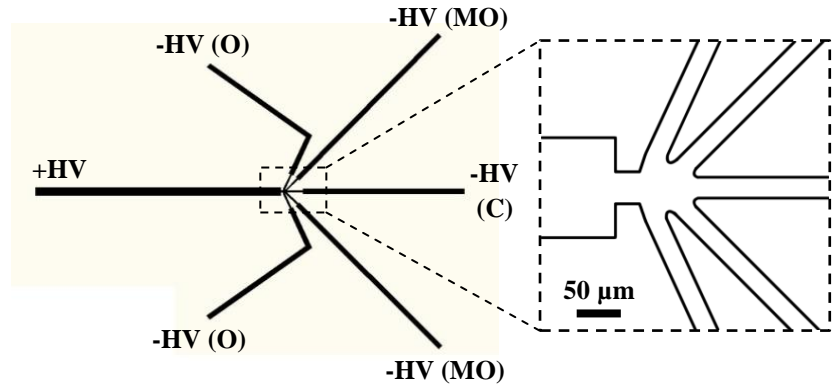


Figure 1: Schematic of entire sorting microstructure and enlargement of restriction region. Positive potential (HV) is applied to inlet on left and negative potential applied to outlets. O: Outer, MO: Mid-Outer, C: Center

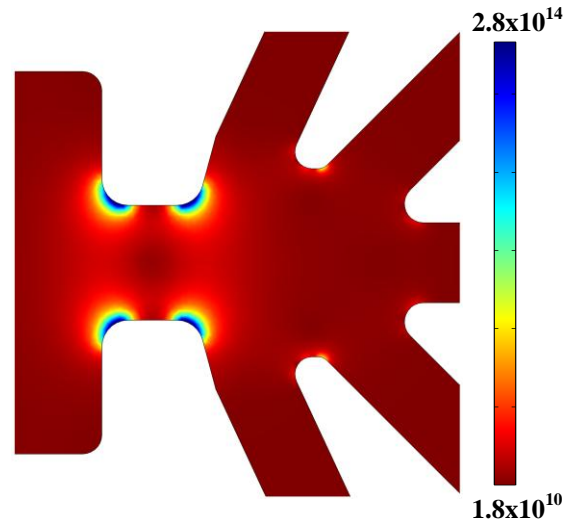


Figure 2:  $\nabla E^2$  in the sorting region. Color bar shows range of values in  $\text{V}^2/\text{m}^3$ .

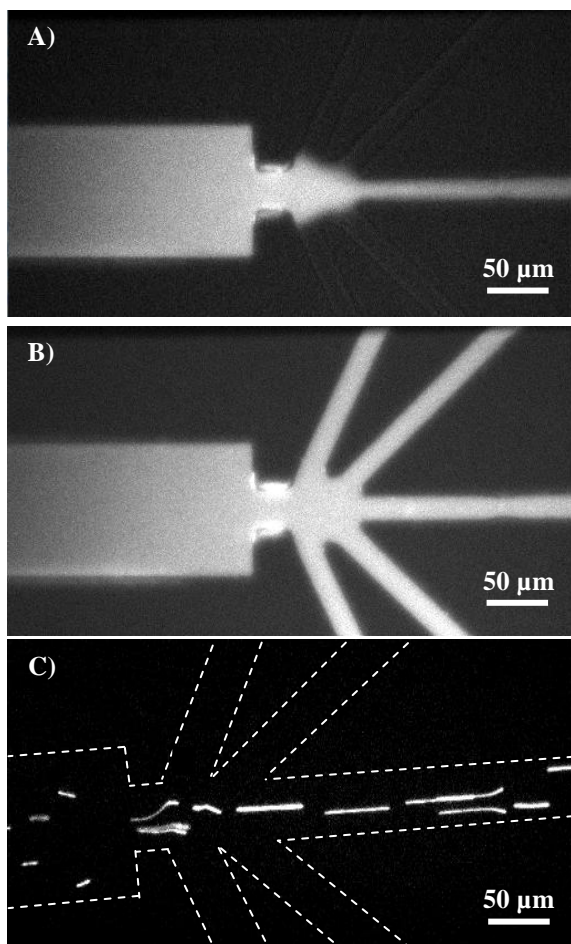


Figure 3: A)  $0.1\ \mu\text{m}$  beads focused at  $>60\text{V}$  applied to center outlet. B)  $0.1\ \mu\text{m}$  beads distributed in all outlets at  $-55\pm 5\text{V}$  applied to the center outlet. C)  $1\ \mu\text{m}$  beads focusing at  $-55\pm 5\text{V}$ .

Conversely, DEP ameliorates the focusing of the  $1\ \mu\text{m}$  beads and thus improves selectivity (Figure 5b) with the same potential scheme applied compared to the case without DEP (Figure 5c) which results in a constant concentration profile for all outlets. These results indicate the importance of balancing DEP and electrokinesis for size fractionation with high selectivity. Our experimental and simulation data indicate that this technique is promising for future applications such as crystal sorting in the field of membrane protein nanocrystallography.

## REFERENCES

- [1] Srivastava, SK. et al. *A continuous DC-insulator dielectrophoretic sorter of microparticles*, J. Chromatogr. A, 1218, pp. 1780-1789, (2011).
- [2] Fromme, P and Spence, JC. *Femtosecond nanocrystallography using X-ray lasers for membrane protein structure determination*, Curr. Opin. Struct. Biol, 21, pp. 509-516, (2011).
- [3] Minerick, A.R. *Encyclopedia of Micro- & Nanofluidics*, Springer, (2008).
- [4] Bhattacharya S. et al. *Insulator-based dielectrophoretic single particle and single cancer cell trapping*, Electrophoresis, 32, pp. 2550–2558, (2011).

## CONTACT

\* Alexandra Ros 1-480-965-5323 or alexandra.ros@asu.edu

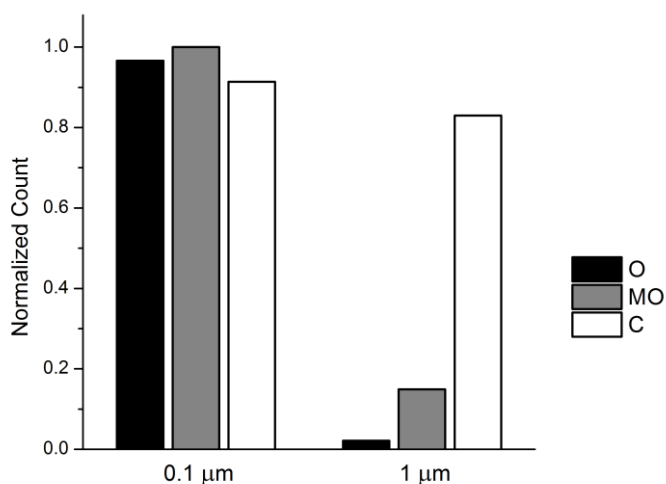


Figure 4: Separation efficiency represented as the normalized ratio of beads flowing into the center outlet with respect to the other outlets.

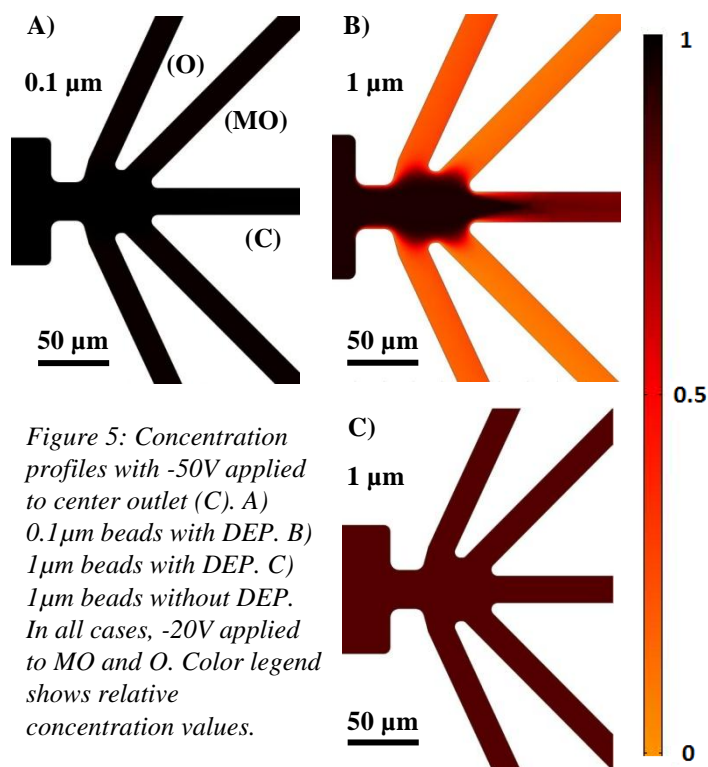


Figure 5: Concentration profiles with  $-50\text{V}$  applied to center outlet (C). A)  $0.1\ \mu\text{m}$  beads with DEP. B)  $1\ \mu\text{m}$  beads with DEP. C)  $1\ \mu\text{m}$  beads without DEP. In all cases,  $-20\text{V}$  applied to MO and O. Color legend shows relative concentration values.